CrossMark

Studies on the adsorption behavior of americium and europium on radiolytically degraded solvent impregnated resin containing neutral and acidic extractants

G. Saipriya[1,3] · R. Kumaresan[2] · P. K. Nayak[2] · K. A. Venkatesan[2] ·
M. P. Antony[2,3] · T. Kumar[1]

Abstract The trivalent actinide selective neutral extractants such as carbamoylmethylphosphine oxide (CMPO) and bis-(2-ethylhexyl)diglycolamide (TEHDGA) in conjunction with an acidic extractant bis-2-ethylhexylphosphoric acid (HDEHP) have been impregnated in Tulsion ADS 400, and the resultant solvent impregnated resin (SIR) has been evaluated for the radiolytic stability towards gamma radiation. The extraction behavior of Am(III) and the loading behavior of Eu(III) in the SIR was studied as a function of absorbed dose up to 550 kGy, at different nitric acid concentrations in aqueous phase. The extraction isotherm of Eu(III) in various SIRs have been fitted using Langmuir, Freundlich, Temkin and Dubinin-Radushkevich (D-R) adsorption models. The extraction results and modeling of extraction isotherms obtained at various absorbed dose levels have been reported in this paper.

Keywords Solvent impregnated resins · Diglycolamide · Organo phosphorus acid · Americium(III) · Europium(III) · Radiolytic degradation · Adsorption isotherms

✉ K. A. Venkatesan
kavenkat@igcar.gov.in

1 Kalpakkam Reprocessing Plant, INRP-K, NRB, Kalpakkam 603102, India

2 Materials Chemistry and Metal Fuel Cycle Group, Indira Gandhi Centre for Atomic Research, Kalpakkam 603102, India

3 Homi Bhabha National Institute, Training School Complex, Anushakti Nagar, Mumbai 400094, India

Introduction

The spent nuclear fuel (SNF) is reprocessed for the recovery of uranium and plutonium. This is carried out by an aqueous based industrially established PUREX process [1]. In this method, the spent nuclear fuel is dissolved in nitric acid medium followed by the solvent extraction of uranium and plutonium in a solution of tri-n-butyl phosphate (TBP) in *n*-dodecane (*n*-DD) [1, 2]. The PUREX raffinate is then concentrated to yield high-level liquid waste (HLLW). It is composed of a solution of stable and radioactive fission products, corrosion products, long lived trivalent actinides (^{241}Am) in 3–4 M nitric acid medium. Partitioning of long-lived trivalent actinides and transmutation of them into stable or short-lived products is proposed for the safe-management of HLLW [3, 4]. Currently, partitioning procedure is a two-cycle solvent extraction method, which involves the group separation of trivalent actinides and lanthanides, together as a group, from HLLW in the first solvent extraction cycle [5–8]. Since the chemistry of trivalent lanthanides is similar to the trivalent actinides, they are also co-extracted as a group in the first solvent extraction cycle. Since the lanthanides act as neutron poisons during the transmutation of actinides, it is necessary to separate actinides from lanthanides or vice versa. This procedure forms the second solvent extraction cycle [5–8]. A number of methods have been reported in literature for group separation, as well as for the lanthanide-actinide separation from high-level liquid waste [9–17].

Among the various techniques reported in literature, solid phase extraction is ideally suited for the separation of small quantities of trivalent metal ions present in a large volume of HLLW [18, 19]. For such separations, the solid phase is usually a macroporous acrylic polymer or

polystyrene-divinyl benzene co-polymer containing the trivalent selective extractants physically adsorbed in the pores of an organic polymer. The solid product obtained after impregnation of extractant is known as solvent impregnated resin (SIR) [20]. Extensive studies have been reported in literature on the separation of trivalent lanthanides and actinides from nitric acid medium using SIRs [18–22]. The advantage of using SIRs for group separation is that there is no concern about third phase formation, which is usually encountered during the solvent extraction of trivalent actinides from nitric acid medium. Among the various neutral extractants reported in literature, the derivatives of carbamoylmethyl phosphine oxide (CMPO) and diglycolamides such as bis-(2-ethylhexyl) diglycolamide (TEHDGA) are considered as promising reagents for the separation of trivalent metal ions from HLLW [9, 16].

Similar to the two-cycle solvent extraction procedure discussed above, the trivalent metal ions can be separated from nitric acid medium by the use of SIR containing CMPO or TEHDGA. The recovery of the loaded trivalents from the loaded SIR is usually carried out with dilute nitric acid, in the first cycle. The recovered product in dilute nitric acid medium is then treated with another SIR containing a suitable reagent for lanthanide-actinide separation in the second cycle. Among the various extractants reported in literature bis- 2-ethylhexylphosphoric acid (HDEHP) is a promising candidate for Ln-An separation from dilute nitric acid medium [23, 24]. In view of the above, the method proposed for trivalent actinide separation using SIR is also a two-cycle extraction-cum-recovery procedure, which involves the group separation of lanthanides and actinides together using a neutral extractant (CMPO or TEHDGA) impregnated resin in the first-cycle followed by Ln–An separation using acidic extractant (HDEHP) impregnated resin in the second cycle.

In order to minimize the generation of secondary waste and simplify the two-cycle process, single-cycle methods using SIRs have been developed [25, 26] for the separation of trivalent actinides alone from the nitric acid medium representing HLLW. This method requires the impregnation of both the neutral extractant and an acidic extractant in a macroporous solid phase. Previously, we studied the extraction behavior of Am(III) and Eu(III) in the SIRs containing a combination of extractants such as CMPO + HDEHP and TEHDGA + HDEHP, and reported the Eu(III) to Am(III) separation factor of 10–15 [25, 26]. The conditions needed for the efficient separation of Eu(III) over Am(III) was optimized and it was proposed to use a combined solvent impregnated resin containing 30 wt% of the neutral extractant (CMPO or TEHDGA) and 10 wt% of HDEHP in the solid phase. When the SIR is proposed for the separation of actinides from HLLW, it is

quite likely that the solvent present in the resin as well as the macroporous matrix could undergo radiolytic degradation. The radiolytic products formed in the resin could combine with each other or combine with the resin matrix (both degraded and undegraded) leading to the formation of several degradation products in the resin phase. The presence of these degradation products could alter the extraction and stripping behavior of Am(III) and Eu(III) from nitric acid medium. In view of this, it is necessary to study the radiolytic stability of the SIR phase containing CMPO + HDEHP and TEHDGA + HDEHP. This can be studied by determining the distribution coefficient and loading behavior of Eu(III) or Am(III) from nitric acid medium in the gamma irradiated SIRs at various absorbed dose levels. Since the extraction of trivalents (An(III) + Ln(III)) from HLLW was carried out from 3 to 4 M and recovery of trivalents from the loaded resin phase was carried out from 0.01 M nitric acid medium [27], the concentration of nitric acid in the present study was fixed at 3 M during extraction, and 0.01 M during stripping. The neutral extractant used in the present study was either CMPO or TEHDGA and an acidic extractant was HDEHP. The composition of neutral and acidic extractant in the SIR was optimized to be 30 and 10 wt% respectively, based on our previous study [25, 26]. The structures of CMPO, TEHDGA and HDEHP are shown in Fig. 1.

Experimental

Materials and methods

All the reagents used in the present study were of Analytical grade. The extractant TEHDGA was synthesized by the procedure described elsewhere [10]. The preparation involved a two steps process. In the first-step, bis-(2-ethylhexyl) diglycolamic acid was prepared by a reaction between diglycolic anhydride and bis-(2-ethylhexyl) amine in dichloromethane solvent. The second-step involved the reaction of bis-(2-ethylhexyl) diglycolamic acid and bis-(2-ethylhexyl)amine in presence of dicyclohexylcarbodiimide (DCC) at 308 K. The crude product obtained was purified by column chromatography using ethyl acetate and petroleum ether mixture as solvent [10]. CMPO was procured from National Chemical laboratory, Pune. CMPO was purified by column chromatography using neutral alumina before use. HDEHP was procured from M/s. Sigma Aldrich and used as received. The radioisotope $^{(152+154)}$Eu(III) tracer was procured from Board of Radiation and Isotope Technology, Mumbai, India. ^{241}Am(III) was received from Oak Ridge National Laboratory as Am_2O_3 and dissolved in nitric acid. The concentration of Eu in aqueous phase was

Fig. 1 Structure of extractants
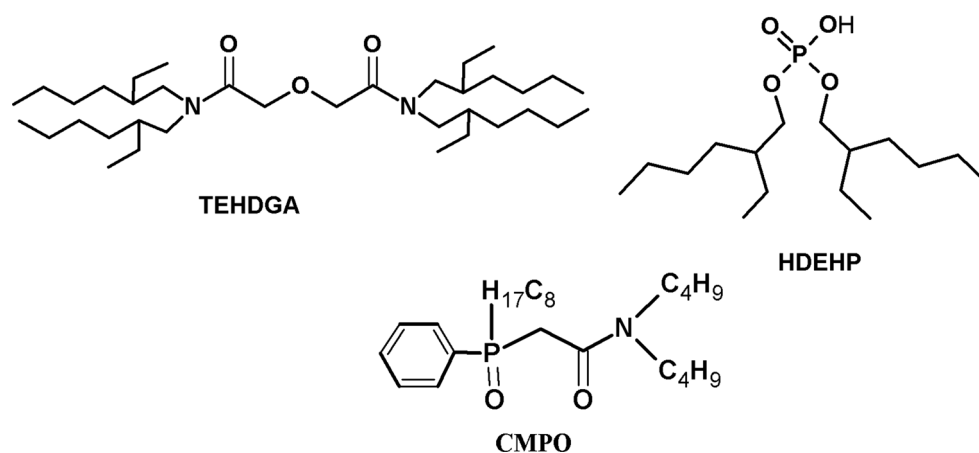
analyzed by Ultima C spectroanalyser (Jobin Yvon, France) equipped with ICP excitation source.

Preparation of solvent impregnated resins (SIRs)

Tulsion ADS 400 was used as a solid support for the impregnation of extractants. Tulsion ADS 400 is a macro porous acrylic polymer with an average particle size 600 μm. The surface area of the dry resin was about 400 m^2/g. The monomers present in the Tulsion ADS 400 was removed by washing in sequence with water, methanol and acetone, and dried at 353 K under vacuum. The required quantity of CMPO or THEDGA or HDEHP or CMPO + HDEHP or TEHDGA + HDEHP was dissolved in dichloromethane and equilibrated with required quantity of Tulsion ADS 400. The mixture was shaken in a vortex shaker for about 8 h. After shaking, the dichloromethane was removed slowly by rotary evaporator at 353 K. The amount of neutral and acidic extractants present in the SIR was 30 and 10 wt % respectively.

Distribution coefficient measurements

All experiments were carried at 298 K. The distribution coefficient of Am(III) and Eu(III) was determined by batch equilibration procedure. About 0.05 g of the SIR was equilibrated with 5 mL of aqueous phase containing desired concentration of nitric acid spiked with $^{(152+154)}$Eu(III) or ^{241}Am(III) tracer. The mixture was taken in 15 mL capacity stoppered glass tube and it was immersed in the constant temperature water bath. The tubes were rotated in an up-side-down rotation at a speed of about 50 rpm for 3 h. After equilibration, the resin phase was allowed to settle and an aliquot (1 mL) was taken from the aqueous phase. The radioactivity of ^{241}Am or $^{(152+154)}$Eu present in the aqueous phase was measured using a well-type NaI(Tl) detector. The radioactivity in resin phase was determined indirectly by computing the

difference in the initial and final radioactivity of ^{241}Am or $^{(152+154)}$Eu present in aqueous phase before and after equilibration, respectively. The distribution coefficient (K_d) of Am(III) and Eu(III) was determined using Eq. 1.

$$K_d \ (mL \ g^{-1}) = \left(\frac{A_0 - A_f}{A_f}\right) \times \left(\frac{v}{m}\right) \qquad (1)$$

where A_0 and A_f are the initial and final radioactivity of aqueous phase. v is the volume of aqueous sample (5 mL), and m is the mass (0.05 g) of the sorbent.

Loading isotherm of Eu(III) in SIR was obtained by equilibrating a known weight of SIR (0.05 g) with 3 M nitric acid solution containing various amounts of europium(III) nitrate. The concentration of Eu(III) in aqueous phase was varied from 20 to 550 mg/L. The equilibration was carried out for 3 h. After equilibration, the concentration of europium present in the aqueous phase was determined by ICP-OES. The equilibrium sorption capacity (q_e) was calculated using Eq. 2.

$$q_e = (C_o - C_f) \times \left(\frac{v}{m}\right) \qquad (2)$$

where C_0 and C_f are the initial and final Eu concentrations in aqueous phase. v is the volume of aqueous sample (5 mL), and m is the mass (0.05 g) of the sorbent.

Irradiation experiments

Gamma chamber GC-5000 with ^{60}Co irradiation source supplied by BRIT, India was used for irradiation studies. The dose rate provided by the gamma chamber was 2 kGy/h. The dose rate was calibrated by Fricke dosimeter. All resins were subjected to the cumulative absorbed dose of 25, 50, 100, 200 and 550 kGy. About 20 g of resin was placed in a stoppered reagent bottle (100 mL) and irradiated in a gamma chamber. All the resins were irradiated

under similar conditions. The distribution coefficient of Am(III) and Eu(III) in the irradiated samples was determined, as described above.

Results and discussion

Extraction behaviour of Am(III) and Eu(III) at 3 M nitric acid

The variation in the distribution coefficient of Am(III) from 3 M nitric acid studied as a function of absorbed dose is shown in Fig. 2. The absorbed dose was varied from 1 to 550 kGy and the results were compared with un-irradiated condition (0 kGy). The resin phase contained 30%

Fig. 2 **a** Variation of distribution coefficient of Am(III) & Eu(III) as a function of absorbed dose. **b** Variation of percentage extraction of Am(III) & Eu(III) as a function of absorbed dose. Resins = 30% CMPO/ADS 400 or 30% CMPO + 10% HDEHP/ADS 400, Aqueous phase = 3 M HNO$_3$, $v/m = 100$

CMPO + 10% HDEHP or 30% CMPO. Since, the extraction behavior of trivalent metal ion from 3 M nitric acid medium is predominantly governed by the neutral extractant, the distribution coefficient of Am(III) and Eu(III) in the binary SIR was compared only with the neutral extractant impregnated resin. It can be seen that the distribution coefficient of Am(III) decreases with increase of absorbed dose. The K_d value of Am(III) decreases from 760 to 480 mL/g in case of 30% CMPO SIR and, from 450 to 350 mL/g in case of 30% CMPO + 10% HDEHP SIR, with the increase of absorbed dose from 0 to 550 kGy. It should be noted that the distribution coefficient of Am(III) in CMPO SIR is higher than that observed for CMPO + HDEHP SIR at 3 M nitric acid. This could be due to the antagonistic effect of combining CMPO with HDEHP for the extraction of Am(III) from 3 M nitric acid medium. Figure 2 b shows the variation in the percentage extraction of Am(III) as a function of absorbed dose. Since the percentage extraction is related directly to the distribution coefficient, the percentage extraction of Am(III) also decreases with increase in the absorbed dose. A similar behavior is also observed in the case of Eu(III) extraction in 30% CMPO and 30% CMPO + 10% HDEHP SIR phase as shown in Fig. 2a, b.

The extraction behavior of Am(III) in 30% TEHDGA or 30% TEHDGA + 10% HDEHP SIR at 3 M nitric acid is shown in Fig. 3. The distribution coefficient of Am(III) decreases with increase of absorbed dose in this case also. Since TEHDGA exhibits higher affinity [16, 27] towards trivalent metal ions as compared to CMPO, the distribution coefficient and percentage extraction of Am(III) in SIR phase containing TEHDGA is more as compared to CMPO SIR. A similar behavior also observed in case of Eu(III) extraction in TEHDGA and TEHDGA + HDEHP SIR phases as shown in Fig. 3. The distribution coefficient of Am(III) and Eu(III) decreases from 2250 and 6000 mL/g to 1400 and 2700 mL/g respectively, with the increase of absorbed dose from 0 to 550 kGy in case of 30% TEHDGA SIR. Since the addition of HDEHP to TEHDGA SIR phase lowers [27] the distribution coefficient of Am(III) and Eu(III) due to antagonistic effect, the K_d value of these metal ions in the TEHDGA + HDEHP SIR phase is lower than that observed in TEHDGA SIR as shown in Fig. 3. Moreover, the decrease in the distribution coefficient of Am(III) and Eu(III) is very sharp in the initial period of irradiation up to 100 kGy (approx) absorbed dose, thereafter the variation in the distribution coefficient as a function of absorbed dose is only marginal. The distribution coefficients observed for Eu(III) in TEHDGA and TEHDGA + HDEHP are very close to each other when the absorbed dose is 500 kGy.
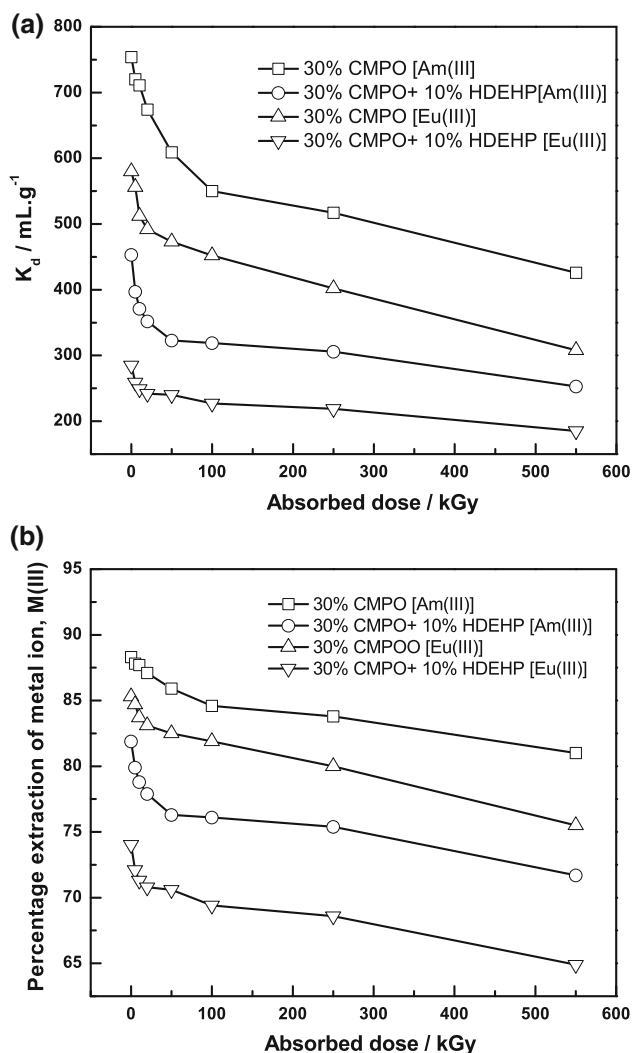
Fig. 3 **a** Variation of distribution coefficient of Am(III) & Eu(III) as a function of absorbed dose. **b** Variation of percentage extraction of Am(III) & Eu(III) as a function of absorbed dose. Resins = 30% TEHDGA/ADS 400 or 30% TEHDGA + 10% HDEHP/ADS 400, Aqueous phase = 3 M HNO$_3$, v/m = 100
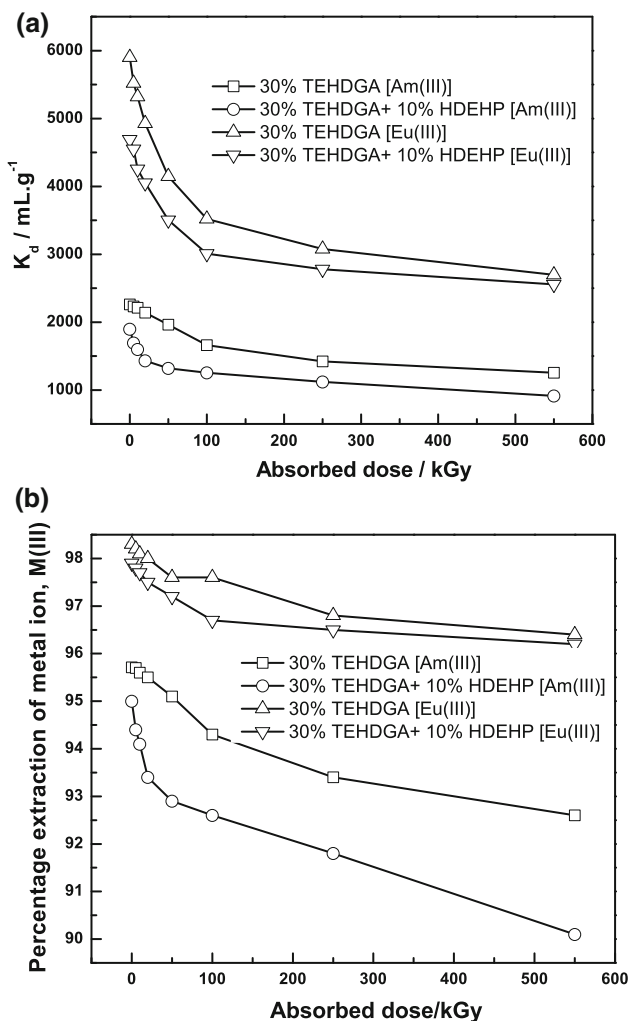

Fig. 4 **a** Variation of distribution coefficient of Am(III) & Eu(III) as a function of absorbed dose. **b** Variation of percentage extraction of Am(III) & Eu(III) as a function of absorbed dose. Resins = 30% CMPO/ADS 400 or 30% CMPO + 10% HDEHP/ADS 400, Aqueous phase = 0.01 M HNO$_3$, v/m = 100

Extraction behavior of Am(III) and Eu(III) at 0.01 M nitric acid

The extraction behavior of trivalent metal ion at lower nitric acid (0.01 M) in the binary SIR is essentially governed by the acidic extractant. Therefore, the distribution coefficient of Am(III) and Eu(III) in the binary SIR was compared only with HDEHP impregnated resin. Figure 4 shows the variation in the distribution coefficient of Am(III) in 30% CMPO + 10% HDEHP SIR at 0.01 M nitric acid determined as a function of absorbed dose. The data are compared with those obtained in 10% HDEHP SIR. It can be seen that the distribution coefficient of Am(III) decreases with increase in the absorbed dose in both cases. Since the presence of CMPO in HDEHP SIR enhances [25] the extraction of Am(III) due to synergism,
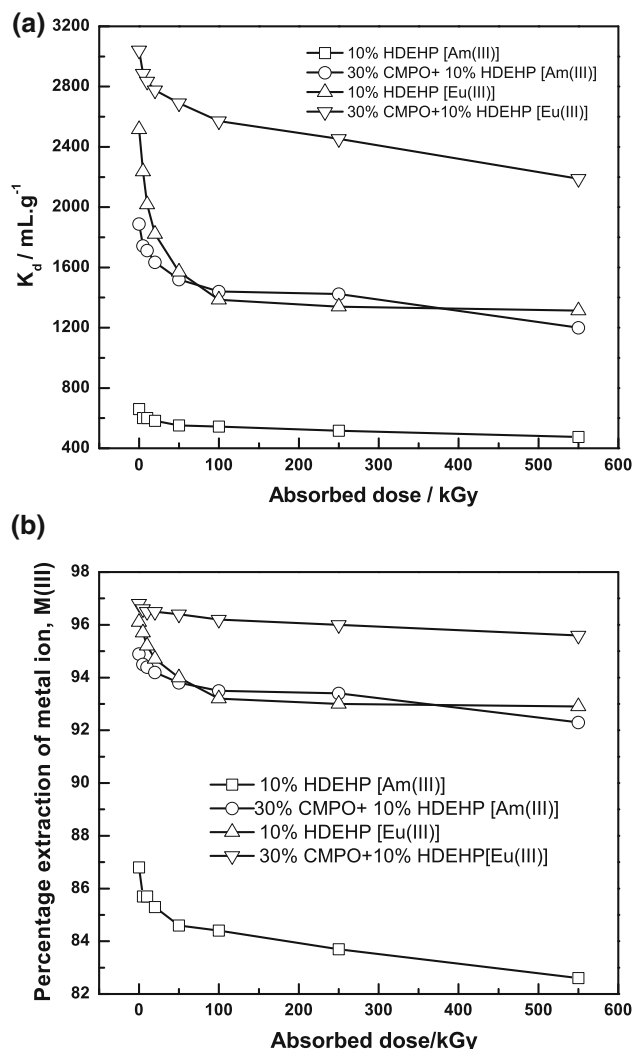
the distribution coefficient of Am(III) in CMPO + H-DEHP is more as compared to HDEHP SIR. A similar behavior is also observed for the extraction of Eu(III) in CMPO + HDEHP and HDEHP SIR, as shown in Fig. 4. However, the distribution coefficient of Eu(III) is always higher than those observed for Am(III) under similar conditions, at all absorbed dose levels. In addition, the distribution coefficient observed for Eu(III) in un-irradiated SIR is about 2–3 times higher than those observed for Am(III).

The variation in the distribution coefficient of Am(III) and Eu(III) as a function of absorbed dose in 10% HDEHP and 30% TEHDGA + 10% HDEHP SIR at 0.01 M nitric acid is shown in Fig. 5. It can be seen that distribution coefficient of Am(III) and Eu(III) decreases with increase
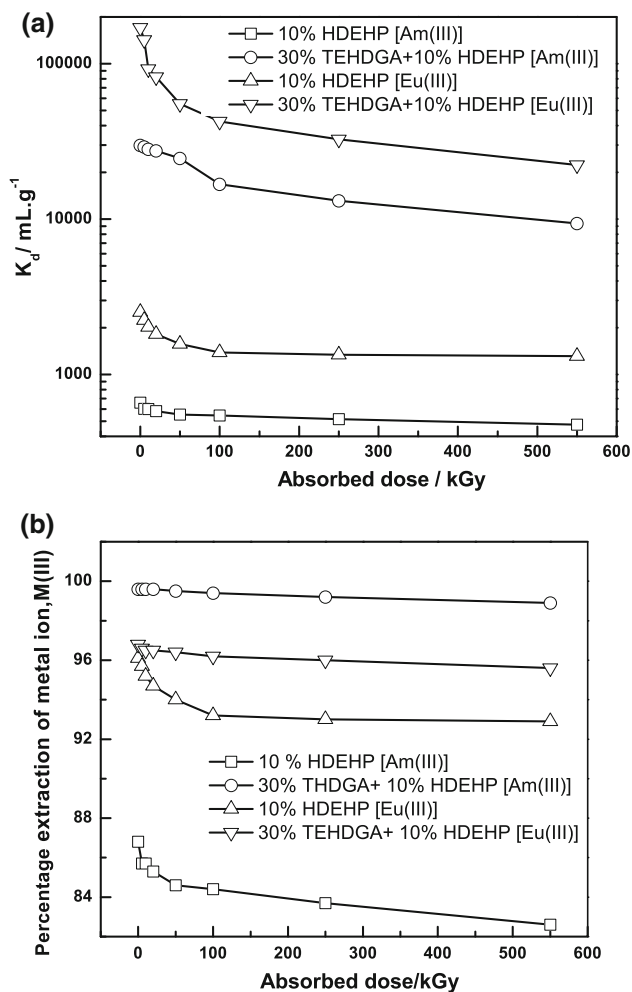
(a)

(b)

Fig. 5 a Variation of distribution coefficient of Am(III) & Eu(III) as a function of absorbed dose. **b** Variation of percentage extraction of Am(III) & Eu(III) as a function of absorbed dose. Resin = 30% TEHDGA/ADS 400 or30% TEHDGA + 10% HDEHP/ADS 400, Aqueous phase = 0.01 M HNO$_3$, v/m = 100

of absorbed dose as expected. Since TEHDGA is a tridentate ligand (Fig. 1) and strongly binding ligand as compared to the bidendate CMPO, the distribution coefficients of Am(III) and Eu(III) observed in the presence of TEHDGA at 0.01 M nitric acid are much higher than those observed in case of CMPO + HDEHP SIR at all absorbed dose levels. In view of this, the distribution coefficient of Am(III) and Eu(III) observed in TEHDGA + HDEHP SIR is much higher than 10000 mL/g even at the absorbed dose of 550 kGy; where as in CMPO + HDEHP SIR it is nearly 2000 mL/g.

Separation factor of Eu(III) over Am(III)

Table 1 shows the separation factor of Eu(III) over Am(III) achieved in all SIRs as a function of absorbed dose at 3 M and 0.01 M nitric acid. It can be seen that the variation in

the SF of Eu(III) over Am(III) as a function of absorbed dose is quite insignificant at 3 M nitric acid. In CMPO SIR the SF remains at a constant value of 0.75 at all absorbed dose levels even though the distribution coefficients decrease with increase of absorbed dose. Addition of HDEHP to CMPO SIR decreases the SF to some extent at 0 kGy and the SF increases marginally with increase of absorbed dose. In case of TEHDGA SIR, the SF decreases marginally with increase of absorbed dose. Addition of HDEHP to TEHDGA SIR decreases the SF to some extent at 0 kGy and the SF increases marginally with increase of absorbed dose. Nevertheless, the variation in the separation factors at 3 M nitric acid are not quite significant as the extraction of Am(III) and Eu(III) at 3 M nitric acid are controlled essentially by the neutral extractant.

The SF of Eu(III) over Am(III) achieved at 0.01 M nitric acid is also shown in Table 1. Since the distribution coefficient of trivalent metal ion is predominantly controlled by HDEHP at 0.01 M nitric acid, the SF of Eu(III) over Am(III) obtained in HDEHP SIR at 0.01 M nitric acid is also shown in Table 1. It can be seen that the SF decreases marginally from 3.8 to 2.7 with increase of absorbed dose in HDEHP SIR. Even though the presence of CMPO increased the distribution coefficient of Am(III) and Eu(III), as shown in Figs. 4 and 5, the SF decreased from 3.8 to 1.6 for the un-irradiated CMPO + HDEHP SIR. The SF then increases marginally from 1.6 to 1.8. In contrast to this, the presence of TEHDGA increases the SF of Eu(III) over Am(III) for the un-irradiated TEHDGA + HDEHP SIR and then the SF decreases with increase in the absorbed dose.

Adsorption isotherms

The variation in the loading behaviour of Eu(III) in resin phase as a function of equilibrium concentration of Eu(III) in aqueous phase can be described by adsorption isotherms. The adsorption behavior of Eu(III) was further evaluated by fitting of the isothermal adsorption data into various models such as Langmuir [28, 29], Freundlich [30], Dubinin-Radushkevich [31, 32, 33] and Temkin isotherms [34]. Each adsorption model provides an insight into the nature of adsorption and the interaction happening between the adsorbent and adsorbate. In addition, the useful parameters such as apparent experimental capacity of the adsorbent and energy of adsorption can also be determined from adsorption models. It should be noted that the adsorption isotherms were initially developed for describing the adsorption behavior of gases on solid surfaces and most often they were also utilized for describing the adsorption behaviour of metal ions from aqueous solution on solid surfaces.

Table 1 Variation in the separation factor of Eu(III) over Am(III) at 3 M and 0.01 M nitric acid. Resins = 30% CMPO + 10% HDEHP, 30% TEHDGA + 10% HDEHP, 30% CMPO, 30% TEHDGA, 10% HDEHP (un-irradiated and irradiated up to 550 kGy)

Dose (kGy)	SF at 3 M nitric acid in				SF at 0.01 M nitric acid in		
	CMPO	CMPO + HDEHP	TEHDGA	TEHDGA + HDEHP	HDEHP	CMPO + HDEHP	TEHDGA + HDEHP
0	0.77	0.63	2.61	2.47	3.82	1.61	5.71
5	0.77	0.65	2.47	2.68	3.72	1.65	4.90
10	0.72	0.67	2.40	2.66	3.36	1.65	3.27
20	0.73	0.69	2.30	2.83	3.13	1.70	2.90
50	0.78	0.74	2.11	2.65	2.84	1.77	2.24
100	0.82	0.71	2.12	2.40	2.55	1.78	2.53
250	0.78	0.71	2.17	2.50	2.60	1.72	2.50
550	0.72	0.73	2.15	2.80	2.76	1.82	2.37

Langmuir adsorption isotherm

Among the various adsorption models, the Langmuir model [28, 29] is the simplest form of adsorption isotherm employed for describing the adsorption data: It is based on the assumption that the adsorbent surface is homogeneous in terms of energy of adsorption and there is no migration of adsorbate across the surface. It also assumes that the maximum adsorption corresponds to mono-layer adsorption of the adsorbate, usually applicable for gaseous adsorption on solid surfaces. The non-linear expression for describing the Langmuir adsorption isotherm is shown in Eq. 3.

$$q_e = \frac{q_m K_L C_e}{1 + K_L C_e} \tag{3}$$

where q_e (in mg/g) is the equilibrium concentration of the adsorbate on the adsorbent, q_m is the maximum concentration of the adsorbate on the solid phase at equilibrium, K_L is the Langmuir adsorption constant that determines the affinity of the adsorbent towards the adsorbate, and C_e (mg/mL) is the equilibrium concentration of the adsorbate. At high concentration of C_e the value of q_m tends to approach the value q_e, i.e. the apparent adsorption capacity equal to the equilibrium concentration of the adsorbate on the adsorbent, according to Eq. 3.

Freundlich adsorption isotherm

It was initially proposed as an empirical model [30] for describing the adsorption of gaseous molecules on solid surfaces, applicable in several cases. Later, Sips et al. [30] theoretically interpreted the insight of the Freundlich model and provided physical significance to the adsorption isotherm. This model assumes that the surface of the adsorbent was heterogeneous and therefore the energy of adsorption was not uniform. The non-linear form of Freundlich adsorption model is represented by the relation shown in Eq. 4.

$$q_e = K_f C_e^{1/n} \tag{4}$$

where K_f (mL/g) is the Freundlich adsorption constant, 'n' represents the degree of heterogeneity of the surface. When $1/n$ is equal to 1, the surface is said to be homogeneous (similar to Langmuir) and the value lower than unity represents heterogeneous nature of surface.

Dubinin-Radushkevich (D-R) isotherm

The physical or chemical nature of interactions happening between the adsorbent and adsorbate can be determined from the D-R adsorption model [31, 32]. The non-linear form of D-R model is represented in Eq. 5.

$$q_e = q_m \exp\left(-K_{DR}\left[RT \ln\left(1 + \frac{1}{C_e}\right)\right]^2\right) \tag{5}$$

$$q_e = q_m \exp\left(-K_{DR}\varepsilon^2\right) \tag{6}$$

where K_{DR} is the D-R constant, ε is known as the Polanyi potential, R is the gas constant and T is the temperature in Kelvin. The D-R constant, K_{DR} is related to the mean free energy of adsorption E (in kJ/mole) by Eq. 7.

$$E = \frac{1}{\sqrt{2K_{DR}}} \tag{7}$$

Depending upon the value of E, the nature of adsorption can be classified [33] into physical or chemical adsorption. When the value of E is lower than 8 kJ/mole, the interac-
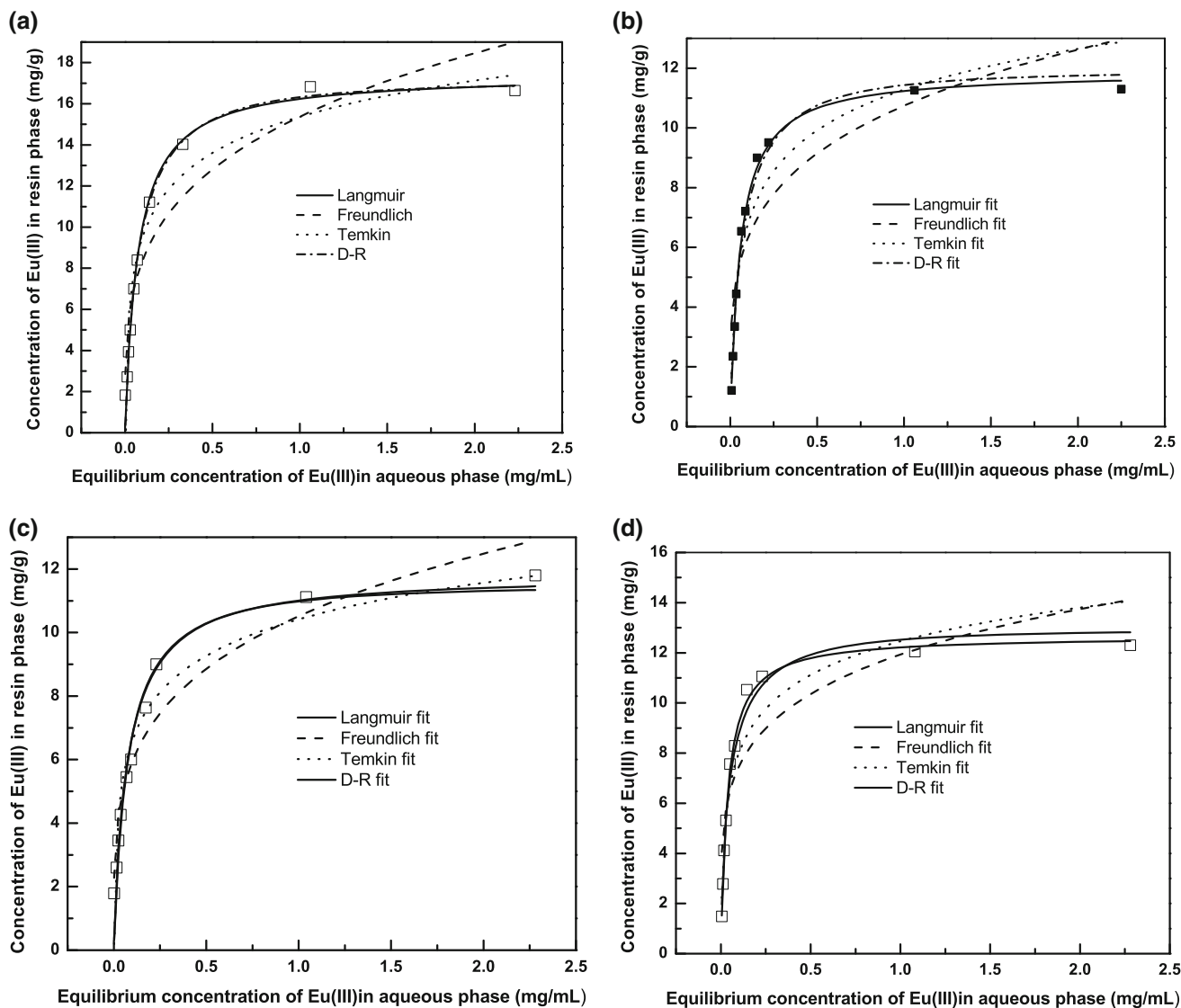
Fig. 6 The non-linear fitting of various adsorption isotherm models. a Un-irradiated 30% CMPO + 10% HDEHP/ADS 400 resin, b 550 kGy irradiated 30% CMPO + 10% HDEHP/ADS 400 resin, c un-irradiated 30% CMPO/ADS 400 resin, d 550 kGy irradiated 30% CMPO/ADS 400 resin, Aqueous phase = 3 M nitric acid

tion happening between the adsorbent and adsorbate is considered as physical interaction and if it is more than 8 kJ/mole, the interaction is chemical in nature. However, it should be noted that this is applicable for gases adsorption on solid surfaces.

Temkin isotherm

The Temkin isotherm considers only the chemical interactions happening between the adsorbate and adsorbent. The model assumes that the energy of adsorption of the adsorbate on the surface decreases linearly with coverage

rather than logarithmically. The non-linear expression for the Temkin model is shown in Eq. 8.

$$q_e = \left(\frac{RT}{b}\right)\ln\alpha + \left(\frac{RT}{b}\right)\ln C_e \tag{8}$$

where b is the variation in adsorption energy and α is the binding constant corresponding to the maximum binding energy.

The adsorption isotherm of Eu(III) on all SIRs were determined and the variation in the loading behavior Eu(III) as a function of Eu(III) concentration in aqueous
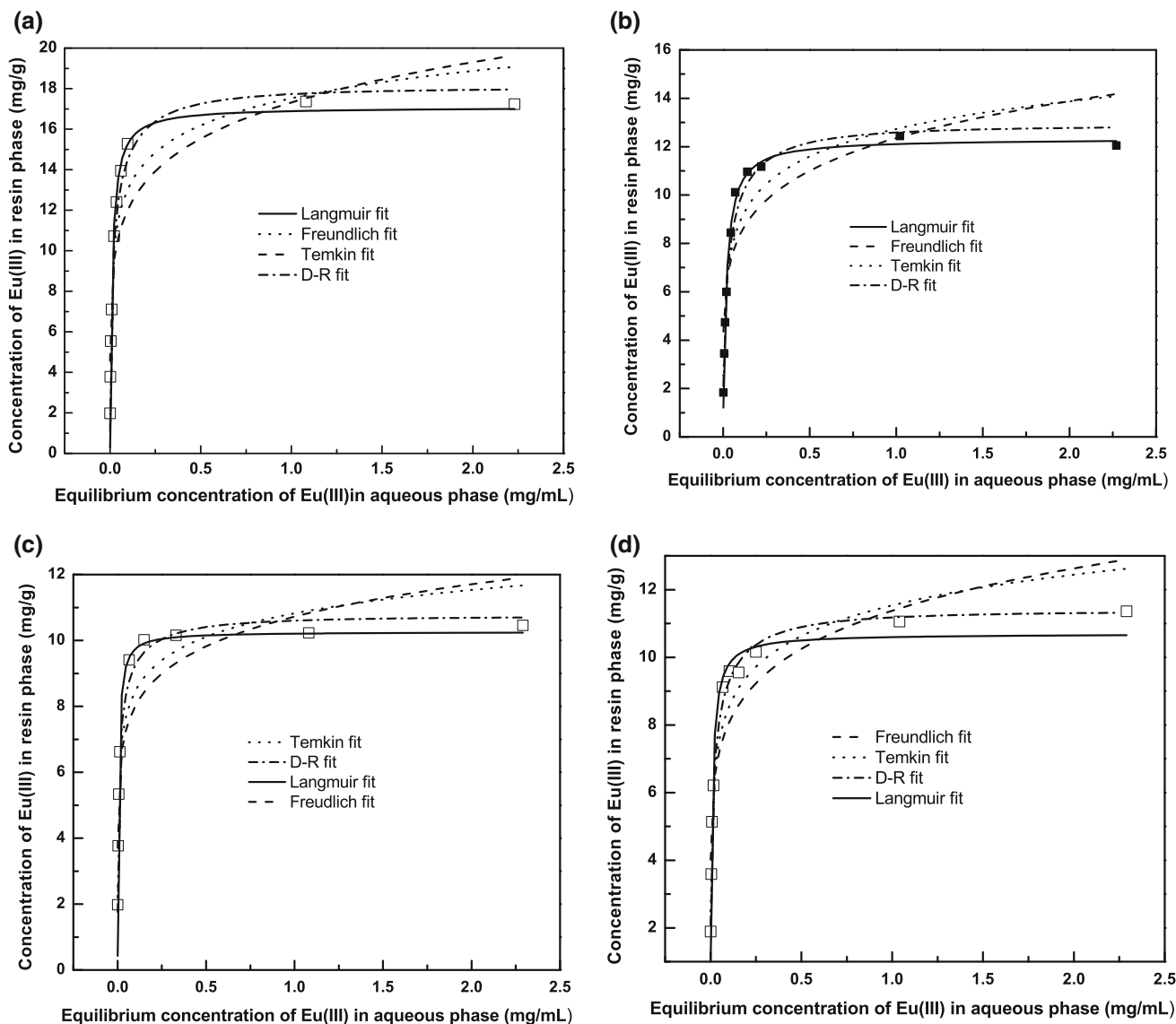
Fig. 7 The non-linear fitting of various adsorption isotherm models. **a** Un-irradiated 30% TEHDGA + 10% HDEHP/ADS 400 resin, **b** 550 kGy irradiated 30% TEHDGA + 10% HDEHP/ADS 400 resin\, **c** un-irradiated 30% TEHDGA/ADS 400 resin **d** 550 kGy irradiated 30% TEHDGA/ADS 400 resin. Aqueous phase = 3 M nitric acid

phase is shown in Figs. 6 and 7. Since the concentration of nitric acid in HLLW is in the range of 3–4 M the loading of Eu(III) was studied only at 3 M nitric acid medium. The initial concentration of Eu(III) in aqueous phase was varied from 10 to 500 mg/L. It can be seen from Figs. 6 and 7 that the loading of Eu(III) in the SIR phase increases rapidly with increase in the concentration of Eu(III) in aqueous phase in the beginning of the isotherm and thereafter the variation is gradual leading to saturation. The adsorption data were fitted with various model equations, discussed above and the non-linear fitting of the data are also shown in Figs. 6 and 7. The fitting constants determined from the non-linear curve fitting are displayed in Table 2.

It can be seen from Table 2 that the adsorption data are described well by the Langmuir model with R^2 value > 0.96 in all cases. The apparent experimental capacity of Eu(III) adsorption on the un-irradiated CMPO SIR is about 12 mg/g and its magnitude increased to 17.4 mg/g in the presence of HDEHP i.e. in CMPO + H-DEHP SIR. A similar behavior is also observed for TEHDGA SIR and TEHDGA + HDEHP SIR. It is important to note that the value of K_L, that determines the affinity of Eu(III) towards the adsorbent, is more when TEHDGA is present in the adsorbent as compared to CMPO SIR. In addition, the presence of HDEHP in TEHDGA SIR lowered the value of K_L to a significant extent. Comparing the apparent experimental capacity

Table 2 Fitting constants and statistical parameters obtained from various adsorption isotherms

	Un-irradiated				Irradiated			
	q_m (mg/g)	K_L (mL/mg)	R^2	χ^2	q_m (mg/g)	K_L (mL/mg)	R^2	χ^2
Langmuir adsorption Isotherm								
30% CMPO	11.83	13.36	0.96	0.47	12.67	26.69	0.99	0.07
30% CMPO + 10% HDEHP	17.43	13.50	0.99	0.32	11.9	17.43	0.99	0.066
30% TEHDGA	10.26	187.05	0.96	0.49	10.69	107.53	0.98	0.29
30% TEHDGA + 10% HDEHP	17	86.01	0.98	0.67	12.33	54.17	0.99	0.15
	K_f (mg/g)	$1/n$	R^2	χ^2	K_f (mg/g)	$1/n$	R^2	χ^2
Freundlich adsorption Isotherm								
30% CMPO	10.51	0.25	0.93	0.91	11.92	0.2	0.79	3.68
30% CMPO + 10% HDEHP	15.37	0.26	0.9	3.47	10.74	0.23	0.81	2.87
30% TEHDGA	10.72	0.13	0.83	1.96	11.37	0.15	0.84	1.93
30% TEHDGA + 10% HDEHP	17.31	0.16	0.82	6.27	12.35	0.16	0.78	3.56
	b (kJ/mol)	α (mL/g)	R^2	χ^2	b (kJ/mol)	α (mL/g)	R^2	χ^2
Temkin adsorption isotherm								
30% CMPO	1.5	534	0.94	0.81	1.3	615	0.91	1.55
30% CMPO + 10% HDEHP	0.97	423	0.93	2.48	1.2	307	0.93	1.06
30% TEHDGA	2.4	38194	0.92	0.89	1.8	6633	0.94	0.68
30% TEHDGA + 10% HDEHP	1.3	8523	0.92	2.83	1.5	2318	0.90	1.60
	Q_m(mg/g)	E(kJ/mol)	R^2	χ^2	Q_m(mg/g)	E(kJ/mol)	R^2	χ^2
D-R adsorption Isotherm								
30% CMPO	11.47	5.78	0.97	0.40	12.93	6.75	0.98	0.32
30% CMPO + 10% HDEHP	17	5.68	0.99	0.32	11.91	6.66	0.988	0.18
30% TEHDGA	10.73	10.92	0.988	0.14	11.37	9.30	0.99	0.07
30% TEHDGA + 10% HDEHP	18.04	9.05	0.98	0.51	12.87	8.13	0.98	0.29

The fitting constants obtained for irradiated SIR (550 kGy) are compared with un-irradiated systems

value determined for irradiated and un-irradiated SIRs, it can be seen that the capacity (q_m) was not affected to any significant extent with the increase of absorbed dose in case of CMPO or TEHDGA SIRs. However, in case of CMPO + HDEHP or TEHDGA + HDEHP SIR, the q_m values decreased upon irradiation (550 kGy).

The Freundlich fitting constants obtained from non-linear curve fitting of the experimental data are displayed in Table 2. It can be seen that fitting of the data is not as good as Langmuir model fitting. The R^2 value for Freundlich fitting ranges from 0.78 to 0.93. In the un-irradiated SIR the K_f values increased upon adding the acidic extractant to the neutral extractant present in the resin. However there is no definite sequence in case of irradiated SIR. The values of $1/n$ ranges from 0.13 to 0.26 for both irradiated and un-irradiated SIR indicating the surface is heterogeneous.

The Table 2 also shows the parameters derived from the fitting of the Temkin adsorption model to the experimental data. The adsorption energy b (in kJ/mol) obtained for both un-irradiated and irradiated adsorbent are nearly comparable. Among the various models described above the experimental data were best fitted using the D-R adsorption model. Based on the value of correlation coefficients (R^2 value) and low Chi square value, the Eu(III) adsorption data in irradiated and un-irradiated adsorbents follows the order D-R model > Langmuir > Temkin > Freundlich. The fitting constants obtained for the experimental data using D-R isotherm are displayed in Table 2. It can be seen that the adsorption capacity (q_m) obtained from D-R isotherm is comparable to the value of q_m, obtained from Langmuir model. Moreover, the study shows that the adsorption capacity of the adsorbent was not affected to a significant extent even after irradiation up to 550 kGy absorbed dose as discussed above.

Conclusions

The SIRs containing the neutral and acidic extractants namely CMPO + HDEHP and TEHDGA + HDEHP have been prepared and evaluated for the radiolytic stability of the SIR toward gamma radiation. The SIRs were irradiated up to the absorbed dose level of 550 kGy. The results were compared with gamma irradiated CMPO or TEHDGA or HDEHP SIRs as well as with the un-irradiated SIRs. The extraction of Am(III) in SIR was studied 3 M nitric acid and 0.01 M nitric acid. The distribution coefficient of Am(III) and Eu(III) decreased with increase of absorbed dose. At 3 M nitric acid, the distribution coefficient of these metal ions in the neutral extractant impregnated was higher than that observed in the neutral + acidic extractant impregnated resin due to antagonistic effect. On the other hand, at 0.01 M nitric acid, the presence of neutral extracant along with HDEHP in the resin, enhanced the extraction Am(III) and Eu(III) due to synergism. Since TEHDGA exhibits higher extraction as compared to CMPO, the distribution coefficient of Am(III) and Eu(III) was more whenever TEHDGA was present in the resin phase as compared to CMPO SIR. The loading behavior of Eu(III) as a function of Eu(III) concentration in aqueous phase in various SIRs was fitted using Langmuir, Freundlich, Temkin and D-R models. Based on the statistics of fitting, the Eu(III) adsorption data was best fitted in the following order D-R model > Langmuir > Temkin > Freundlich. The adsorption capacity obtained from D-R isotherm was comparable with the capacity obtained from Langmuir model and the results also revealed that the adsorption capacity was not affected to any significant extent in these SIRs, even at the absorbed dose level of 550 kGy. Therefore, these SIRs can be used for the single cycle separation of Am(III) from high-level liquid waste.

References

1. Herbst RS, Baron P, Nilsson M (2011) Standard and advanced separation: PUREX processes for nuclear fuel reprocessing. In: Nash KL, Lumetta GJ (eds) Advanced separation techniques for nuclear fuel reprocessing and radioactive waste treatment. Woodhead Publishing, Cambridge, pp 141–175. ISBN 978-1-84569-501-9
2. McKay HAC, Miles JH, Swanson JL (1990) Science and technology of tributyl phosphate. In: Schulz WW, Navratil JD (eds) Applications of tributyl phosphate in nuclear fuel reprocessing, vol III, 2 Ed edn. CRC Press, Florida
3. Raj K, Prasad KK, Bansal NK (2006) Radioactive waste management practices in India. Nucl Eng Des 236(7):914–930
4. Salvatores M (2005) Nuclear fuel cycle strategies including partitioning and transmutation. Nucl Eng Des 235(7):805–816
5. Venkatesan KA, Kumaresan R, Antony MP, Kumar T, Srinivasan TG, Vasudeva Rao PR (2012) Characterization of high active waste (155 GWd/Te) arising from fast reactor fuel reprocessing. Radiochimi Acta 100(11):843–850
6. Veliscek-Carolan J (2016) Separation of actinides from spent nuclear fuel: a review. J Hazard Mater 318:266–281
7. Panak PJ, Geist A (2013) Complexation and extraction of trivalent actinides and lanthanides by triazinylpyridine N-donor ligands. Chem Rev 113(2):1199–1236
8. Mathur JN, Murali MS, Nash KL (2001) Actinide partitioning—a review. Solvent Extr Ion Exch 19(3):57–90
9. Philip Horwitz E, Kalina DC, Diamond H, Vandegrift GF, Schulz WW (1985) The TRUEX process-a process for the extraction of the transuranic elements from nitric acid wastes utilizing modified PUREX solvent. Solvent Extr Ion Exch 3(1–2):75–109
10. Sasaki Y, Sugo Y, Suzuki S, Tachimori S (2001) The novel extractants, diglycolamides, for the extraction of lanthanides and actinides in HNO₃–n-dodecane system. Solvent Extr Ion Exch 19(1):91–103
11. Tyumentsev MS, Foreman MR, Ekberg C, Matyskin AV, Retegan T, Steenari BM (2016) The solvent extraction of rare earth elements from nitrate media with novel polyamides containing malonamide groups. Hydrometallurgy 164:24–30
12. Duan W, Wang S, Wang J, Wang J, Chen J (2015) Radioactive tracer tests of two improved trpo processes for high-level liquid waste using annular centrifugal contactors. Solvent Extr Ion Exch 33(2):109–119
13. Braley JC, Grimes TS, Nash KL (2011) Alternatives to HDEHP and DTPA for simplified TALSPEAK separations. Ind Eng Chem Res 51(2):629–638
14. Carrott M, Geist A, Hères X, Lange S, Malmbeck R, Miguirditchian M, Modolo G, Wilden A, Taylor R (2015) Distribution of plutonium, americium and interfering fission products between nitric acid and a mixed organic phase of TODGA and DMDO-HEMA in kerosene, and implications for the design of the "EURO-GANEX" process. Hydrometallurgy 152:139–148
15. Tachimori S, Sasaki Y, Sujuki S (2002) Modification of TODGA-n-dodecane solvent with a monoamide for high loading of lanthanides(III) and actinides(III). Solvent Extr Ion Exch 20(6):687
16. Gujar B, Ansari SA, Mohapatra PK, Manchanda VK (2010) Development of T2EHDGA based process for actinide partitioning. Part I: batch studies for process optimization. Solvent Extr Ion Exch 28(3):350–366
17. Modolo G, Wilden A, Daniels H, Geist A, Magnusson D, Malmbeck R (2013) Development and demonstration of a new SANEX partitioning process for selective actinide (III)/lanthanide (III) separation using a mixture of CyMe4BTBP and TODGA. Radiochim Acta 101(3):155–162
18. Hoshi H, Wei YZ, Kumagai M, Asakura T, Morita Y (2004) Group separation of trivalent minor actinides and lanthanides by TODGA extraction chromatography for radioactive waste management. J. Alloys Compd. 374(1):451–455
19. Mathur JN, Murali MS, Iyer RH, Ramanujam A, Dhami PS, Gopalakrishnan V, Banerji A (1995) Extraction chromatographic separation of minor actinides from PUREX high-level wastes using CMPO. Nucl Technol 109(2):216–225
20. Kabay Nalan, Cortina Jose Luis, Trochimczuk Andrzej, Streat Michael (2010) Solvent-impregnated resins (SIRs)–methods of preparation and their applications. React Funct Polym 70(8):484–496
21. Bhattacharyya AP, Mohapatra K, Manchanda VK (2007) Solvent extraction and extraction chromatographic separation of Am³⁺ and Eu³⁺ from nitrate medium using cyanex® 301. Solvent Extr Ion Exch 25(1):27–39
22. Horwitz EP, McAlister DR, Bond AH, Barrans RE Jr (2005) Novel extraction of chromatographic resins based on tetraalkyldiglycolamides: characterization and potential applications. Solvent Extr Ion Exch 23(3):319–344

23. Nash KL (2015) The chemistry of TALSPEAK: a review of the science. Solvent Extr Ion Exch 33(1):1–55

24. Rama Swami K, Kumaresan R, Nayak P et al (2017) Effect of pKa on the extraction behavior of Am(III) in organo phosphorus acid and diglycolamide solvent system. Radiochim Acta. doi:10.1515/ract-2017-2769

25. Saipriya K, Kumaresan R, Nayak PK, Venkatesan KA, Kumar T, Antony MP (2016) Extraction behaviour of Am(III) and Eu(III) from nitric acid medium in CMPO–HDEHP impregnated resins. Radiochim Acta 104(2):67–75

26. Saipriya G, Kumaresan R, Nayak PK, Venkatesan KA, Kumar T, Antony MP (2016) Extraction behaviour of Am(III) and Eu(III) from nitric acid medium in TEHDGA–HDEHP impregnated resins. Radiochim Acta 104(11):781–790

27. Nayak PK, Kumaresan R, Venkatesan KA, Antony MP, Vasudeva Rao PR (2013) A new method for partitioning of trivalent actinides from high-level liquid waste. Sep Sci Technol 48(9):1409–1416

28. Langmuir I (1918) The adsorption of gases on plane surfaces of glass, mica and platinum. J Am Chem Soc 40(9):1361–1403

29. Langmuir I (1916) The constitution and fundamental properties of solids and liquids. Part I. Solids. J Am Chem Soc 38(11):2221–2295

30. Sips R (1948) On the structure of a catalyst surface. J Chem Phys 16(5):490–495

31. Dubinin M (1960) The potential theory of adsorption of gases and vapors for adsorbents with energetically nonuniform surfaces. Chem Rev 60(2):235–241

32. Saltalı K, Sarı A, Aydın M (2007) Removal of ammonium ion from aqueous solution by natural Turkish (Yıldızeli) zeolite for environmental quality. J Hazard Mater 141(1):258–263

33. Dada AO, Olalekan AP, Olatunya AM, Dada O (2012) Langmuir, Freundlich, Temkin and Dubinin–Radushkevich isotherms studies of equilibrium sorption of Zn2+ unto phosphoric acid modified rice husk. IOSR J Appl Chem 3(1):38–45

34. Temkin MI, Pyzhev V (1940) Kinetics of ammonia synthesis on promoted iron catalysts. Acta Physiochim URSS 12(3):217–222